

Article

Changing Convection in Central Asia during the Seasonal Transitional Period and Region to Its West before and after 1999: Role of Upper Vertical Thermal Contrast

Bakshi Hardeep Vaid

School of Marine Sciences, Nanjing University of Information Science and Technology (NUIST),
Nanjing 210044, China; 002553@nuist.edu.cn; Tel.: +86-15251744283

Abstract: The objective of this study is to investigate and understand the changes in thermal contrast in the upper troposphere over Central Asia before and after 1999. It was observed that there was a discernible increase/decrease in upper tropospheric temperature (TT) in the 100 hPa/250 hPa over the Central Asian region during PRE99, whereas during POST99, it was found to be the other way around. A clear increase and decrease in the upper TT pattern in 100 hPa and 250 hPa can be attributed to anti-cyclonic and cyclonic circulations in the wind shear, respectively. The subtropical jet has been shown to act as a significant dynamical system generating cyclonic circulation over Central Asia, resulting in dynamical features favorable for enhancing convection during PRE99. This is evinced by the structure of the 200hPa zonal winds, which serve as a surrogate for a subtropical jet. It can be seen that the westerly winds over the southern part and the easterly winds over the northern part of Central Asia culminate in a significant cyclonic circulation over the region. In summary, PRE99 showed an increase in convection over Central Asia and the regions to its west. The anatomy, using geopotential height, relative humidity, total cloud area (TCA) fraction, longwave fluxes (LWF), and shortwave fluxes (SWF) through the top of the atmosphere, is consistent with the above results. To further support these findings, an updated and thorough causality analysis is performed, and it is noteworthy to mention that the variation of thermal temperature contrast is found to be causally related to LWF and SWF.

Keywords: upper thermal contrast; seasonal transition period; convection; causal distribution

Citation: Vaid, B.H. Changing Convection in Central Asia during the Seasonal Transitional Period and Region to Its West before and after 1999: the Role of Upper Vertical Thermal Contrast. *Atmosphere* **2023**, *14*, 59. <https://doi.org/10.3390/atmos14010059>

Academic Editors: Jimy Dudhia and Jason C. Kniviel

Received: 1 November 2022

Revised: 19 December 2022

Accepted: 26 December 2022

Published: 28 December 2022



Copyright: © 2022 by the authors. Licensee MDPI, Basel, Switzerland. This article is an open access article distributed under the terms and conditions of the Creative Commons Attribution (CC BY) license (<https://creativecommons.org/licenses/by/4.0/>).

1. Introduction

The monsoon in Central Asia, one of the well-known arid areas in the mid-latitudes, has changed significantly due to climate change [1–7]. From the perspective of climate change, the westerly winds are considered one of the most important features of the region [1,3]. The literature reveals that numerous studies have been conducted to investigate the variability of the monsoon over Central Asia [8–12]. In addition, a variety of factors have been used to explain the variability of the monsoon over Central Asia. For example, sea surface temperature (SST) warming in the tropical Indian Ocean was found to influence the variability of summer precipitation over Central Asia [9]. Evidence of seasonal precipitation over Central Asia closely related to ENSO was proposed [8]. Apart from the oceanic factor, the atmospheric factor was shown to play an important role in the Central Asian monsoon. For example, changes in westerly winds may be the main factor affecting the development of precipitation [10,12–14]. Moreover, research on Central Asia revealed that variations in its humidity are impacted by human-induced warming [11]. Nevertheless, the land signal (the contribution of soil moisture) was also observed to have a significant influence on Central Asia [15].

In particular, it has been documented that dramatic changes in the monsoon can prove catastrophic and that these changes can have significant impacts on regional economies by affecting agricultural, industrial, and hydropower development, as well as the human dimension in the form of health, education, and employment [6,7]. Surprisingly, despite the significance of Central Asia's monsoon, it has not been extensively studied. Apart from this, none of the previous studies worked on the upper thermal contrast, the most dominant parameter impacting climate variability [16–21], and no work has been carried out so far on its dependency on convective activities over Central Asia. Principally, as far as we are aware, the relationship between upper thermal contrast and convection over Central Asia has not been examined previously.

Recently, the importance of upper tropospheric thermal contrast and its impact on convection has provided a new perspective on the monsoon [16–25]. In [26], it was noted that thermal heating of the upper troposphere relative to the lower troposphere is one of the most robust features of the tropics. The upper tropospheric temperature (TT) variability is closely related to the fluctuation of large-scale circulation, and these variations have profound repercussions on a range of environmental factors [16–21,23,27–29]. In addition, the upper TT was observed to impact climate feedback processes and atmospheric dynamics [18,22,23,30–32]. Its effects on upper humidity and upper tropospheric convection are more evident in recent studies [19,20,28,29,33,34]. Given the importance and significance of upper TT [16–25], it would be highly anticipated that a detailed analysis of upper TT over Central Asia and its significance in determining the thermal contrast in the Central Asian region be carried out. Considering these factors, including societal concerns, a detailed investigation of upper TT variability and its concomitance with convection variability over Central Asia is conducted.

We address the upper thermal contrast and its impact on convection over Central Asia during the seasonal transition period that usually occurs in May and June (MJ) [35,36]. The period is generally characterized by rapid changes in general circulation and weather patterns, as well as natural hazards [35,36]. This period is of utmost prominence for a variety of reasons, including the fact that the fluctuations in the dynamics and thermodynamics of the atmosphere during this period can provide a compact, interpretable, and significant predictor of the summer monsoon [16–25,37,38]. Therefore, we predominantly aimed to study the variation of the upper TT and its role in changing convection over Central Asia during this period.

As an overview of the present investigation, this study: (1) identifies a new phenomenon of upper thermal contrast occurring over the Central Asia region during the seasonal transition period; (2) explores the thermal contrast's relationship to the possible dynamical parameters over the region; and (3) utilizes this consideration to examine the thermal contrast's potential to alter convection patterns in the region. The remaining part of this paper is structured as follows. In Section 2, we acquaint ourselves with the data and analysis methods. The upper tropospheric thermal contrast changes and their possible role in changing convection before and after 1999 are presented in Section 3. A corollary of the study is provided in the last section.

2. Materials and Methods

In atmospheric research, reanalysis products are increasingly used to monitor climate change and conduct research in a variety of fields, including climate and energy, taking into account their inherent uncertainties. During the seasonal transition period, we specifically examined the National Center for Environmental Prediction (NCEP) DOE–AMIP 2 daily reanalysis datasets for the period 1982–2017 (<http://www.esrl.noaa.gov/psd/>, accessed on 01 January 2021), which include wind fields, air temperature, geopotential height, and relative humidity. Notably, we particularly employed NCEP version 2 [39] datasets, as prior versions of NCEP [40] data were observed to have large temporal inconsistencies [41]. Recently, NCEP2 has been successfully used

to highlight the decadal variability related to the Asian monsoon [16–25,42–45]. In addition, data from the Modern Era Retrospective analysis for Research and Applications (MERRA) (a project of the Global Modeling and Assimilation Office of NASA) were also used. The MERRA data employed are total cloud area (TCA) fraction, longwave flux (LWF), and shortwave flux (SWF) at the top of the atmosphere [46].

To quantify the effects of the upper TT thermal contrast on the atmospheric variables, such as longwave flux (LWF) and shortwave flux (SWF) over Central Asia and the region towards the west during the seasonal transitional period, we explicitly used recently developed causality between time series [47–50]. To measure the causality between two time series, for example, X_1 and X_2 , we unambiguously applied the Liang–Kleeman information flow method.

The equation is as follows: The highest likelihood estimate of the causality from X_2 to X_1 in the linear limit is:

$$T_{2 \rightarrow 1} = \frac{C_{11}C_{12}C_{2,d1} - C_{12}^2C_{1,d1}}{C_{11}^2C_{12} - C_{11}C_{12}^2} \quad (1)$$

where C_{ij} is the sample covariance between the two time series X_i and X_j ($i, j = 1, 2$), and $C_{i,dj}$ is the covariance between X_i and a derived series.

$$X_j^{\&} = \frac{X_j(t + k\Delta t) - X_j(t)}{k\Delta t} \quad (2)$$

i.e., a series formed from $X_j(t)$ by taking Euler forward differencing, with Δt being the time step size and $k \geq 1$ being some integer (for more details, refs. [20,47–50]). Specifically, to tackle the issue at hand, we have adopted a modified version of an approach described in [20] called “composite causality analysis” for this investigation. Among many others, see [20,47–50], for further niceties on the methodology and applications. Note, ref. [20] provides an enlightening yet succinct introduction from the user’s point of view.

3. Results

This study analyzes the periods 1982–1998 (hereafter PRE99) and 1999–2017 (hereafter POST99) separately because of the recognized dramatic changes in global and regional temperatures before and after 1999 [16,17,51,52]. Interestingly, these distinctions were reported to have affected the convection pattern before and after 1999 [17]. Figure 1 shows the May–June (MJ) averaged TT for the periods PRE99 (a,e) and POST99 (b,f) at 100 hPa and 250 hPa, respectively. The difference (here, a,b) is illustrated in Figure 1c, and a Student’s *t*-test was used to determine its statistical significance (Figure 1d). Similarly, Figure 1g,h correspondingly indicates the differences (here, Figure 1e,f) and their statistical significance. In short, MJ PRE99–POST99 is observed to be significantly different from zero at the 99% confidence level based on a Student’s *t*-test (Figure 1d,h). It is exhibited that throughout the PRE99 and POST99 periods, there was a significant change in TT at 250 hPa and 100 hPa. Positive anomalies at 100 hPa and negative anomalies at 250 hPa (the region’s Long. = 54° E–85° E, Lat. = 22° N–38° N; hereafter Vertical Thermal Contrast region or Region I), respectively, reveal a precise vertical dipole structure over Central Asia (Figure 1c,g). Unambiguously, over the two separate periods, the air temperature at 100 hPa and 250 hPa changed by around 2.5 K and 1 K, respectively. PRE99 minus POST99 cases were shown to have a much warmer/colder upper troposphere at 100/250 hPa (Figure 1c,g), whereas POST99 minus PRE99 displays the reverse structure (Figure not shown). Remember that the case POST99 minus PRE99 is essentially the reverse case of PRE99 minus POST99, which is why we have refrained from showing the figure for the case POST99 minus PRE99 throughout the paper, although a discussion of it was unavoidable. The anatomy in Figure 1 supports the striking difference between the upper thermal contrast in PRE99 and POST99.

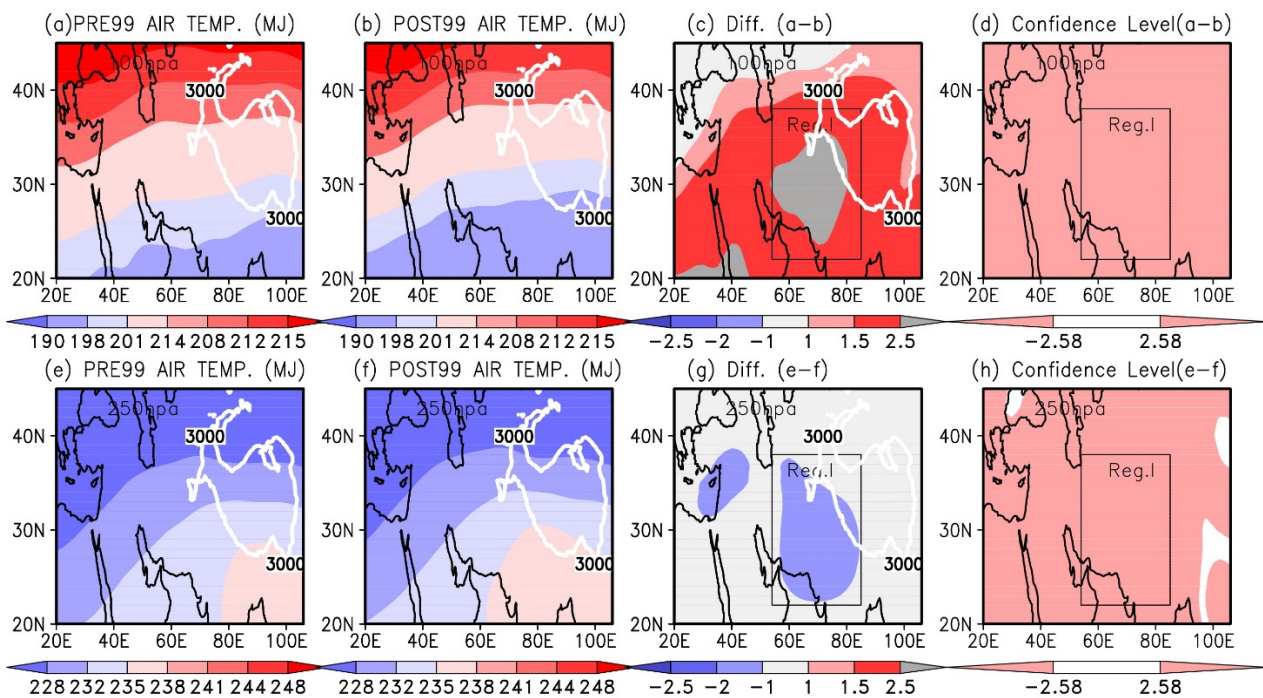


Figure 1. MJ TT (in K) over 100 hPa for the PRE99 (a) and POST99 (b) periods. (c) What separates (a) from (b), i.e., (a) - (b). (d) regions (shaded) showing that (c) is significantly different from zero at a 99% level. (e–h) is like (a–d) but for 250 hPa level. The white contour denotes the topography isoline of 3000 m.

Next, taking into account the role that the upper tropospheric thermal contrast plays in the monsoon system [22–25], we hypothesized that the revealed upper vertical thermal contrast over Central Asia may modulate the monsoon circulation as well as convection over the region and the surrounding area. To determine the upper thermal contrast changes, the MJ TT at 250 hPa is subtracted from that at 100 hPa. The results for PRE99, POST99, and PRE99 minus POST99 for Region I are shown in Figure 2a–c. Over Central Asia, an analysis of the upper vertical thermal contrast during the seasonal transition period suggests a wide range of differences between the different episodes (i.e., PRE99 and POST99), as well as a close relationship between the two. In general, it has been demonstrated that the upper vertical thermal contrast during the seasonal transition period varies by approximately 3K to 6K between the two episodes (i.e., PRE99 and POST99) over Central Asia.

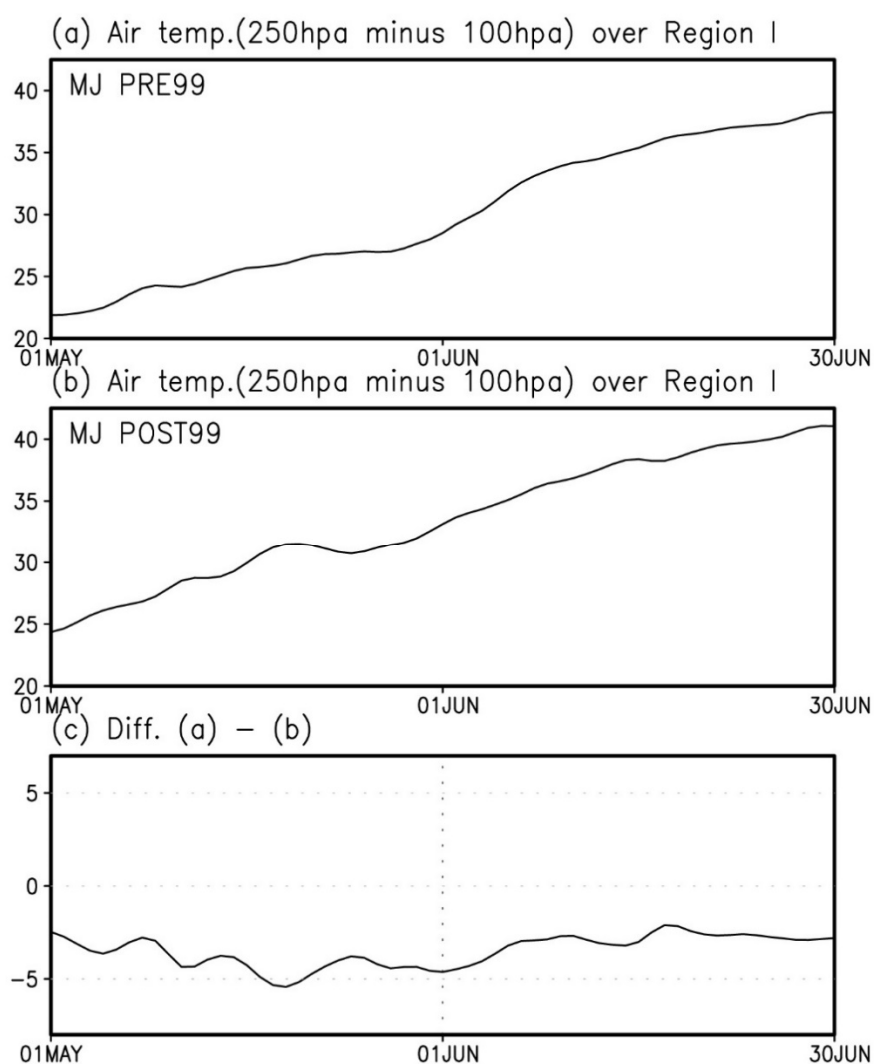


Figure 2. MJ (250 hPa - 100 hPa) air temperature over Region I for (a) PRE99 and (b) POST99. (c) The difference between (a) and (b), or (a) - (b).

It is critical to remember that prior research indicates that upper TT variabilities greater than 0.1–0.3 K are considered to be of substantial importance in climate change studies and their climate drivers [22–25,53,54]. Next, the vertical profiles of the average air temperature for PRE99 and POST99 between the pressure levels 400 hPa to 50 hPa, and their difference between PRE99 and POST99 during MJ, were plotted to further demonstrate the existence of upper vertical thermal contrast over the upper atmosphere (Figure 3c). The disparities show a precise vertical thermal contract of the order of 3 K (Figure 3c). When PRE99 minus POST99 is investigated, the upper troposphere at 100 hPa and 250 hPa is observed to be warmer and colder, respectively. In light of the relationship between thermal contrast and convection [22–25], and its ability to modulate convection patterns [17,55,56], the present study projects that the above observed variation will eventually exert influence on the Central Asian region and its surroundings based on the upper TT variations.

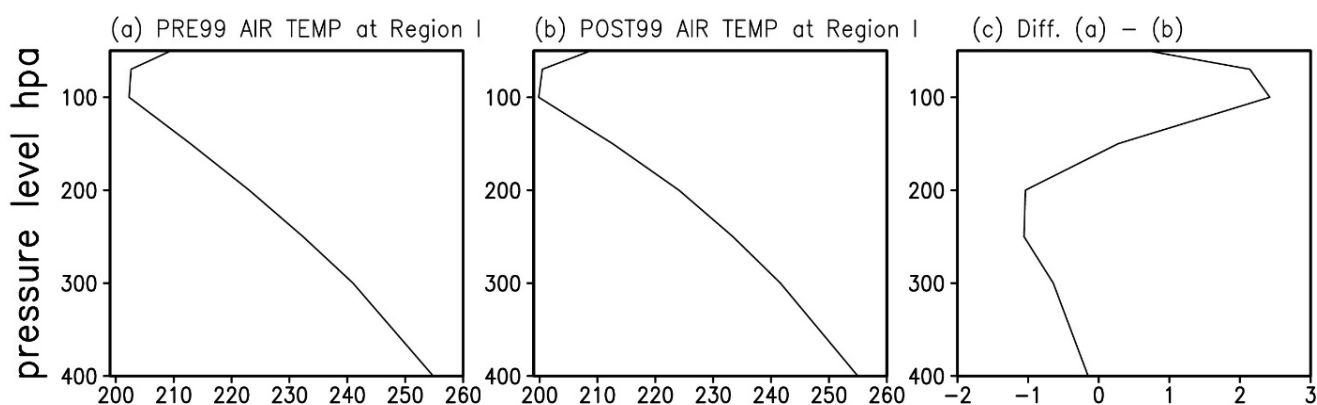


Figure 3. Vertical air temperature changes over Region I (a) PRE99 and (b) POST99. (c) The difference between (a) and (b), specifically, (a) - (b).

The upper tropospheric circulation may alter before and after 1999, as we will see in the subsequent section. The MJ PRE99 minus POST99 wind vector shear anomalies are shown in Figure 4a,b. These are obtained by subtracting the wind vectors at 100 hPa from those at 50 hPa (Figure 4a), and those at 250 hPa from those at 200 hPa (Figure 4b). The illustration demonstrates a precise anomalous cyclonic circulation and an anomalous anti-cyclonic circulation at 250 hPa and 100 hPa, respectively. Even though cyclonic circulation is predominant over region I, as a result of the presence of TT over that region, it has also been shown to dominate the western region of Central Asia. The evidence implies that the out-of-phase vertical change of TT over Central Asia, as seen in Figure 1c,g, and the circulation patterns are related. In short, this is effectively reflected by the structures that have been presented in Figures 1g and 4b.

An analysis of the wind shear indicates an interaction between anomalous cyclonic circulation at 250 hPa and anomalous anti-cyclonic circulation at 100 hPa over the Central Asian region, implying a sign of convection during PRE99 minus POST99. Recollect that the essential force that drives convection over a particular region is the vertical variation of wind [57]. For further details regarding the interaction between anomalous cyclonic circulation and anomalous anti-cyclonic circulation, and its association with convection, please refer to [19,21,57]. This development points to the role of vertical TT interaction in strengthening convection in the case of PRE99 minus POST99 (Figure 4a,b). Overall, it may be suggested that temperature characteristics, in tandem with the circulation (Figures 1g and 4b), constitute the thermodynamical and dynamical cause of the increase and/or decrease in convection before and after 1999, respectively, over Central Asia.

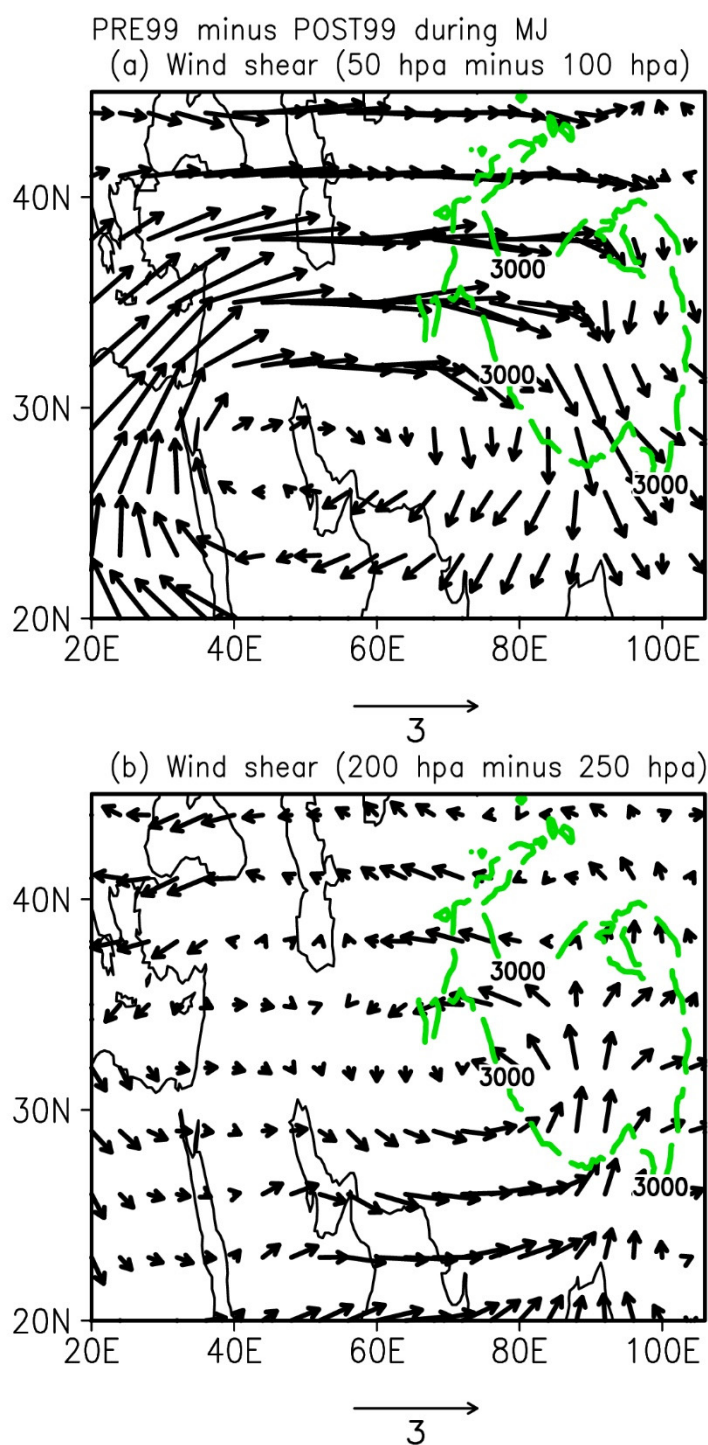


Figure 4. MJ averaged wind shear (in m/s) around 100 hPa and 250 hPa during PRE99 minus POST99 (a) 50 - 100 hPa; (b) 200 - 250 hPa.

Knowing that geopotential height demonstrates the amount of effort made against gravity to raise a unit mass and indicates the capacity of air mass to be lifted, we conducted a geopotential height analysis. The exercise’s debriefing lends support to the idea that convection increases and decreases before and after 1999, respectively (Figure 5c). Negative and positive anomalies in geopotential height can be delineated below and above 100 hPa, respectively, from the plot of PRE99 minus POST99 (Figure 5c). The ability of air mass to be raised from below 100 hPa is demonstrated to be high during the PRE99

minus POST99 period (Figure 5f), and this is in agreement with the aforementioned outcomes (Figures 1g and 4b). Accordingly, geopotential height during PRE99 minus POST99 is observed to be accompanied by an increase in relative humidity (Figure 5f). Notably, in the PRE99 minus POST99 case, a relative humidity increase of around 10% is revealed. A small variation in relative humidity in the upper troposphere may be crucial to the radiative forcing [33]. Around 10% change, for instance, might result in around 1.4 Wm^{-2} change in radiative forcing [19,33,34].

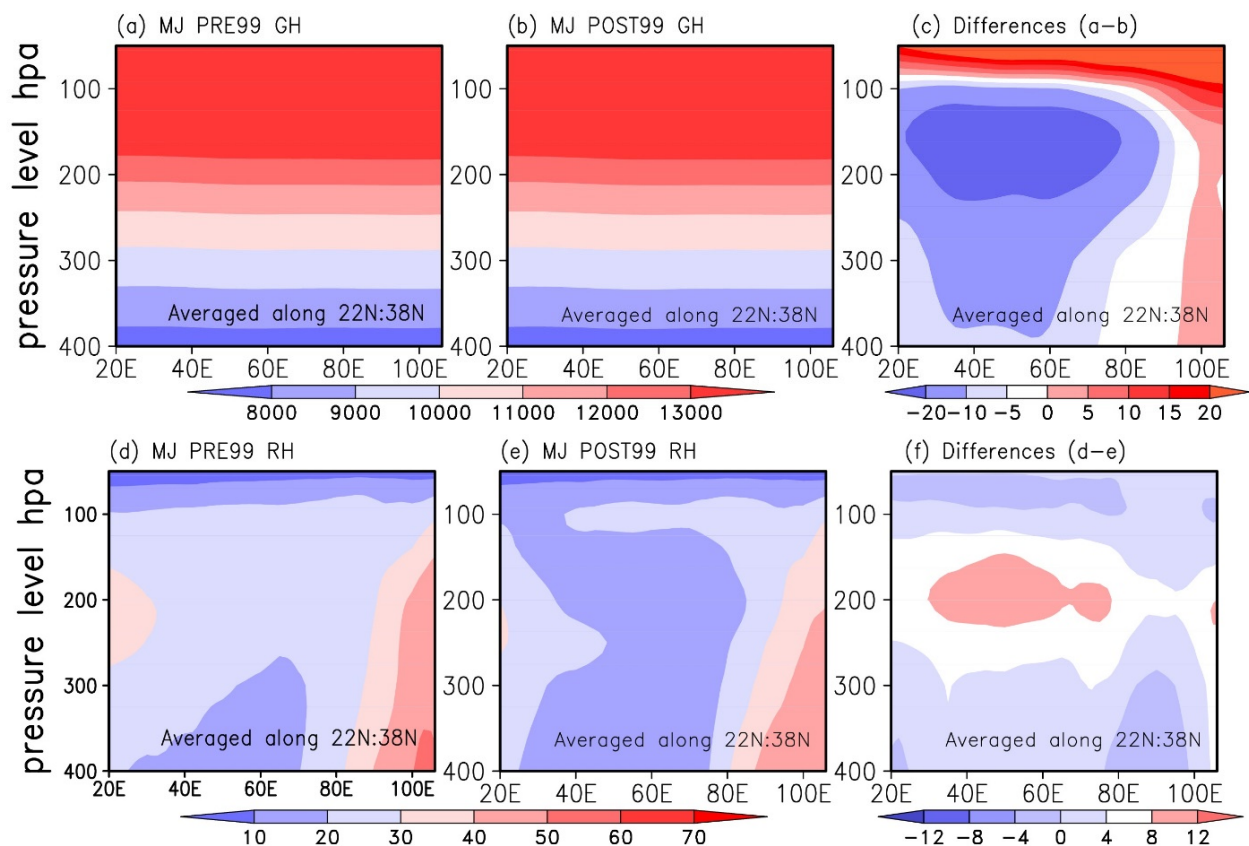


Figure 5. Vertical variation in the geopotential height over the latitudinal band 22° N – 38° N (a) PRE99 and (b) POST99. (c) The difference between (a,b), that is, (a–b). (d–f) as in (a–c), but for relative humidity.

Now, to see the convection changes, the surplus (PRE99 minus POST99) upward LWF, downward SWF, and total flux were plotted at the top of the atmosphere (Figure 6a–c). The findings are further supported by the fact that the longwave flux (LWF) and shortwave flux (SWF) in PRE99 minus POST99 during the seasonal transition period also exhibit consistent fluctuations. In addition to this, we also examined the total cloud area fraction in the PRE99 minus POST99 period. A clear indication of cloud cover is shown in Figure 6d, which is congruent with the PRE99 and POST99 debate (recall here, if the cloud fraction is around 0.01, the sky is considered cloudy; see [58]).

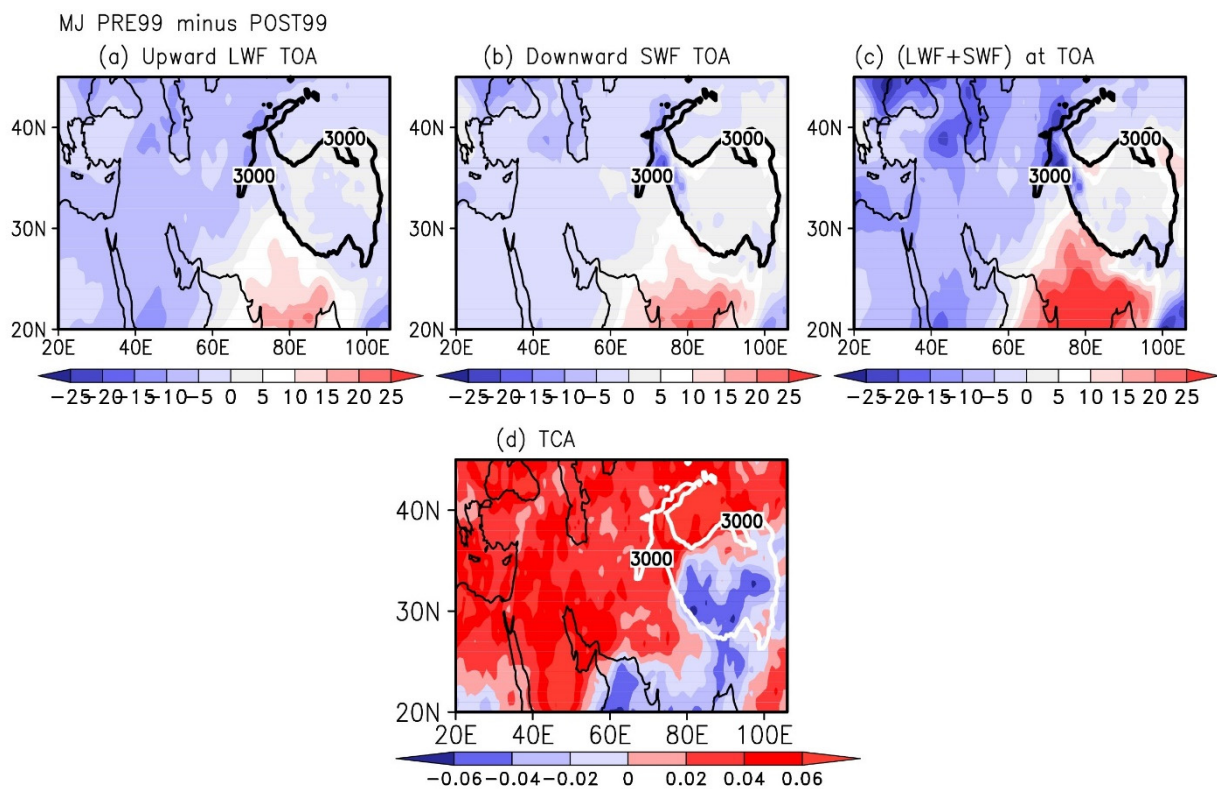


Figure 6. (a) The top of atmosphere MJ mean upward LWF (Wm^{-2}) during PRE99-POST99, (b) as in (a), but for downward SWF; and (c) is the same as (a), but for LWF + SWF. (d) TCA fraction during PRE99 - POST99.

In the subsequent section, we explored the subtropical jet, a prominent dynamical mechanism that was observed to impact the Asian monsoon [21,59,60], and how it related to the changing dynamics over Central Asia. PRE99 minus POST99 shows westerly winds over the southern part in conjunction with easterly winds over the northern part of the Central Asian region (Figure 7c). This signage advocates the development of a cyclonic circulation over Central Asia in support of convection. Implicitly, the observed 200 hPa zonal wind pattern (Figure 7c) indicates a cyclonic circulation in Central Asia. Such potential physical processes should be interpreted as an indication of convection over Central Asia (Figures 4b and 7c). This is supported by the aforementioned conclusions, which indicate that in the case of PRE99 minus POST99, the dynamics and thermodynamics over the Central Asian region cause an increase in convection. Therefore, we conclude that the upper troposphere's dynamics and thermodynamics play a role in the convection manifestations that occur across Central Asia during the seasonal transition period (Figures 1g, 4b, and 7c).

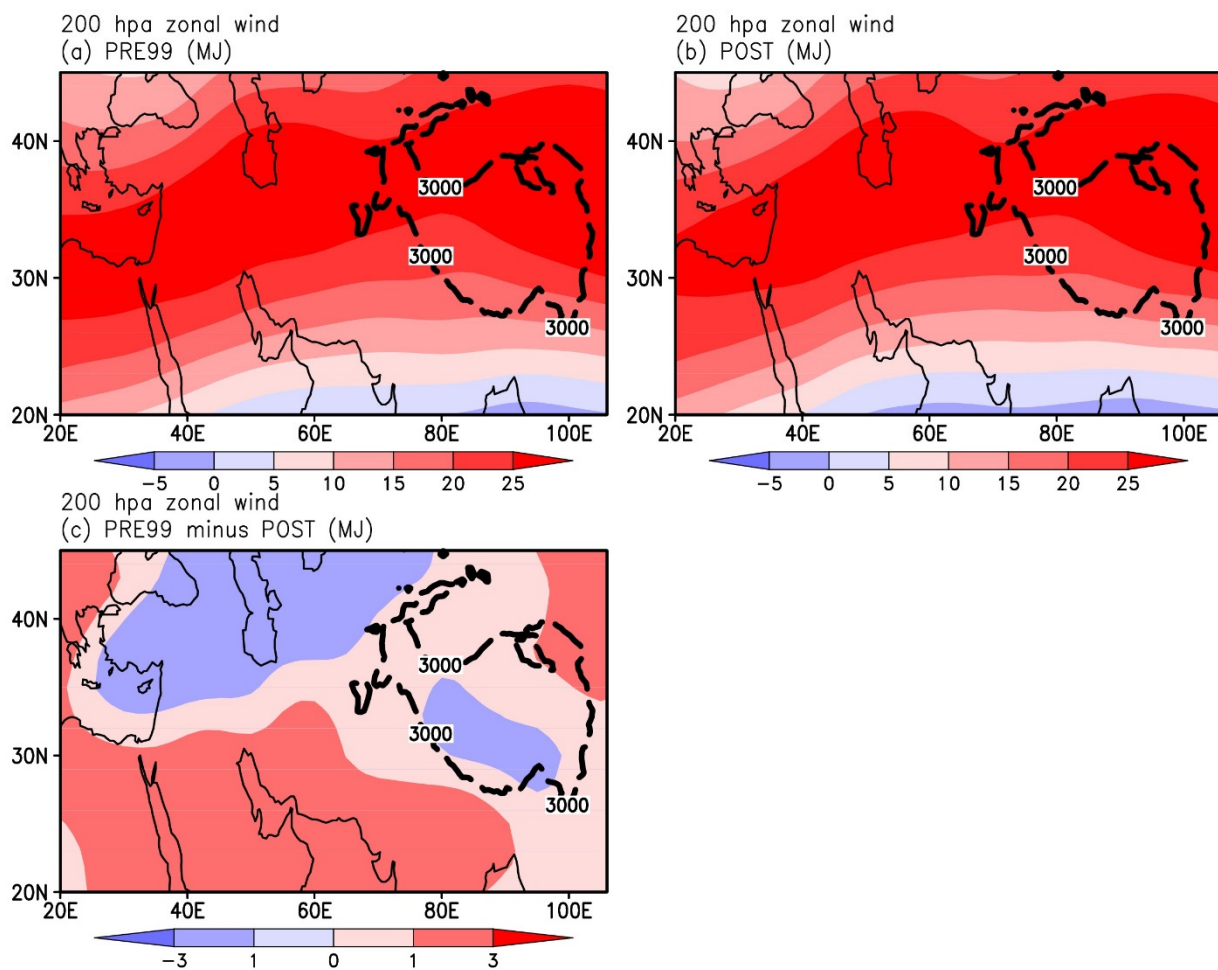


Figure 7. MJ zonal wind at 200 hPa (in m/s) (a) PRE99, (b) POST99, and (c) the difference between the two (i.e., MJ PRE99 - POST99). The 3000 m topographic isoline is shown by the dashed contour.

To strengthen the claim made, the direct relationship of the upper TT variation to LWF and SWF is investigated. The association is quantified using a recently created “composite causality analysis.” The causal patterns generated by various time window sizes, such as 41, 51, 61, and 71 days, were applied; however, the resulting causal patterns are similar. For more details on “composite causality analysis”, please refer to [20]. The results are presented in Figure 8. Causation from the upper TT thermal contrast to LWF and SWF at the top of the atmosphere is measured in nats/day. Nat is the unit for entropy, which has the form of $-\int \rho \log \rho$ (ρ is the pdf; probability density function) when the base of the logarithm is e. The analysis demonstrated that the upper TT variation over the region I was identified to be significantly casual to LWF and SWF over the Central Asian region and the area to its west (Figure 8). It is critical to emphasize that the causalities discovered in this way are asymmetric in direction; specifically, they are derived from the upper TT thermal contrast to the LWF and SWF and are unrelated to those obtained from the other direction. This remarkable observation distinguishes the impact of the upper vertical TT thermal contrast over the region I on the convection changes in PRE99 and POST99.

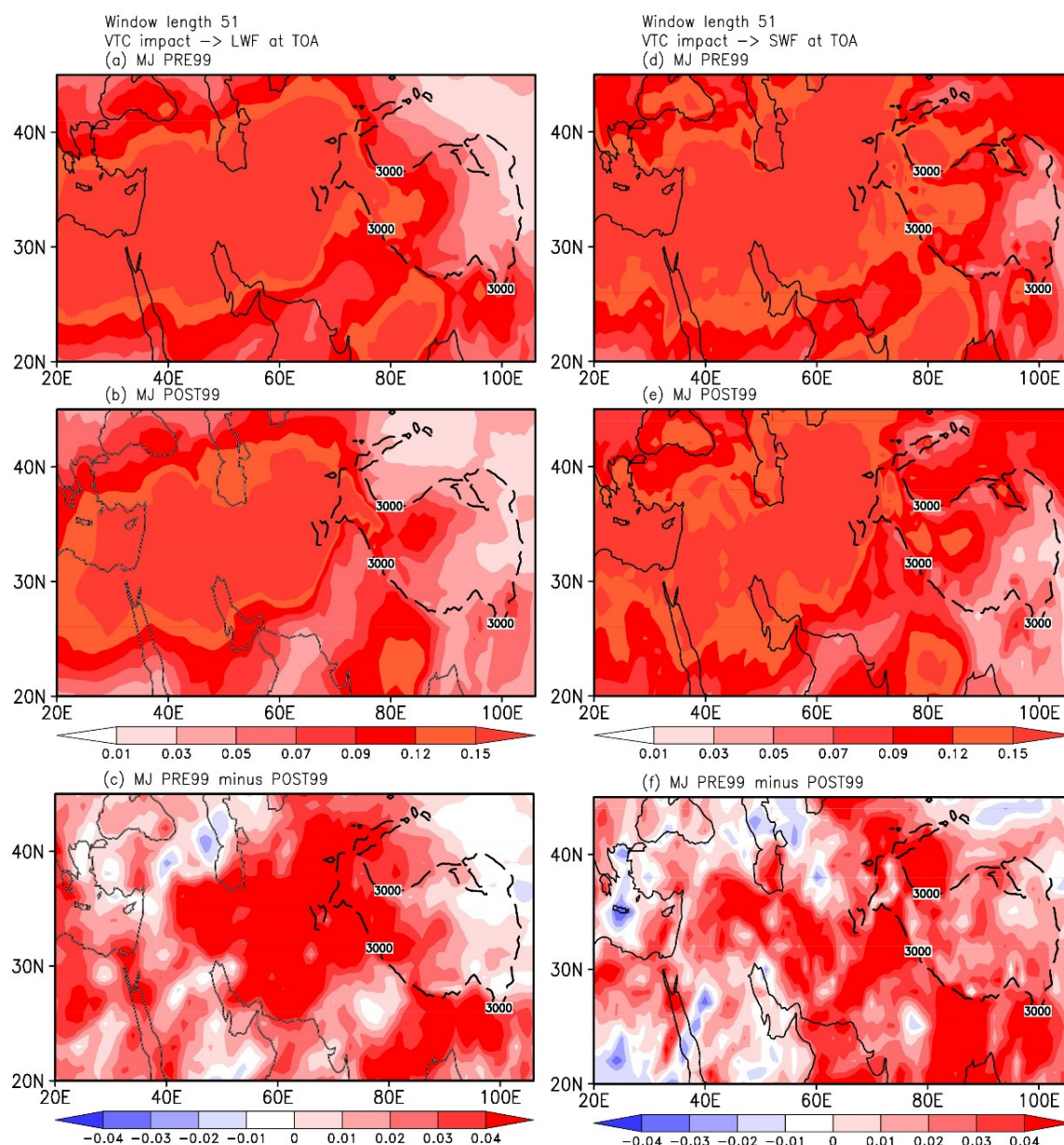


Figure 8. The causation (information flow in nats/day) from the TT thermal contrast (i.e., MJ Air temperature 250 hPa - 100 hPa) over Region I to LWF at the top of the atmosphere for the time windows size of 51 (a) PRE99 and (b) POST99, respectively. (c) Difference (a) from (b), i.e., (a) - (b). The selections (d–f) are identical to (a–c), but SWF was chosen rather than LWF.

4. Discussion

Convection reversal over Central Asia in POST99 was attributed to an upper tropospheric thermal contrast during the seasonal transition period. Studies show that the upper TT over Central Asia in POST99 increased and decreased at 250 hPa and 100 hPa, respectively. This remarkable change in upper thermal contrast is consistent with the change in circulation and longwave and shortwave fluxes at the top of the atmosphere. During POST99, there was an anomaly of anti-cyclonic circulation in the upper troposphere over Central Asia when the upper tropospheric temperature was warmer at 250 hPa. The upper troposphere temperature at 250 hPa was cooler during PRE99, resulting in cyclonic circulation at 250 hPa. The subtropical jet has been shown to contribute signif-

icantly to the cyclonic and anti-cyclonic circulation over Central Asia, leading to dynamical features that influenced convection during PRE99 and POST99, respectively. Based on this physical process, it has been shown that the upper TT over Central Asia is directly relevant to convection over the region. To obtain valid evidence for the effect of the temporal variation of the upper TT on convection over Central Asia and the region to the west of it, we performed a new causality analysis. It confirmed our results. As for the causal inferences, there seems to be a dominant causal relationship between the upper TT gradient over Central Asia and the long- and shortwave fluxes through the upper atmosphere. In short, over Central Asia and regions west of it, the upper TT has been shown to influence convection. Nevertheless, this study supports the idea that convection over Central Asia is influenced by the vertical thermal contrast of the upper troposphere. However, there is a possibility that climatic extremes in other regions of Asia may influence convection over Central Asia. Future studies need to apply sensitivity tests with climate models for precise results, and use short- and long-term predictions to investigate whether convection over Central Asia has global implications.

Funding: This work is supported by the National Science Foundation of China (42230105, 41975064).

Institutional Review Board Statement: Not applicable.

Informed Consent Statement: Not applicable.

Data Availability Statement: The datasets generated during and/or analyzed during the current study are available from the corresponding author upon reasonable request. The datasets used are from MERRA and NCEP-DOE AMIP 2 Reanalysis Version 2.

Acknowledgments: The author is grateful to the editor and the anonymous reviewers for their valuable comments and suggestions, which helped to improve the manuscript in its present form. GrADS was used to visualize the data.

Conflicts of Interest: The authors declare no conflict of interest.

References

1. Huang, W.; Chen, F.H.; Feng, S.; Chen, J.H.; Zhang, X.J. Interannual Precipitation Variations in the Mid-Latitude Asia and Their Association with Large-Scale Atmospheric Circulation. *Chinese Sci. Bull.* **2013**, *58*, 3962–3968. <https://doi.org/10.1007/s11434-013-5970-4>.
2. Hu, Z.; Zhang, C.; Hu, Q.; Tian, H. Temperature Changes in Central Asia from 1979 to 2011 Based on Multiple Datasets. *J. Clim.* **2014**, *27*, 1143–1167. <https://doi.org/10.1175/JCLI-D-13-00064.1>.
3. Huang, W.; Chen, J.; Zhang, X.; Feng, S.; Chen, F. Definition of the Core Zone of the “Westerlies-Dominated Climatic Regime”, and Its Controlling Factors during the Instrumental Period. *Sci. China Earth Sci.* **2015**, *58*, 676–684. <https://doi.org/10.1007/s11430-015-5057-y>.
4. Xu, L.; Zhou, H.; Du, L.; Yao, H.; Wang, H. Precipitation Trends and Variability from 1950 to 2000 in Arid Lands of Central Asia. *J. Arid Land* **2015**, *7*, 514–526. <https://doi.org/10.1007/s40333-015-0045-9>.
5. Hu, Z.; Zhou, Q.; Chen, X.; Qian, C.; Wang, S.; Li, J. Variations and Changes of Annual Precipitation in Central Asia over the Last Century. *Int. J. Climatol.* **2017**, *37*, 157–170. <https://doi.org/10.1002/joc.4988>.
6. Jiang, J.; Zhou, T.; Chen, X.; Zhang, L. Future Changes in Precipitation over Central Asia Based on CMIP6 Projections. *Environ. Res. Lett.* **2020**, *15*, 054009. <https://doi.org/10.1088/1748-9326/ab7d03>.
7. Zhang, M.; Yu, H.; King, A.D.; Wei, Y.; Huang, J.; Ren, Y. Correction to: Greater Probability of Extreme Precipitation under 1.5 °C and 2 °C Warming Limits over East-Central Asia (Climatic Change, (2020), 162, 2, (603–619), 10.1007/S10584-020-02725-2). *Clim. Change* **2020**, *162*, 621. <https://doi.org/10.1007/s10584-020-02792-5>.
8. Chen, X.; Wang, S.; Hu, Z.; Zhou, Q.; Hu, Q. Spatiotemporal Characteristics of Seasonal Precipitation and Their Relationships with ENSO in Central Asia during 1901–2013. *J. Geogr. Sci.* **2018**, *28*, 1341–1368. <https://doi.org/10.1007/s11442-018-1529-2>.
9. Zhao, Y.; Zhang, H. Impacts of SST Warming in Tropical Indian Ocean on CMIP5 Model-Projected Summer Rainfall Changes over Central Asia. *Clim. Dyn.* **2016**, *46*, 3223–3238. <https://doi.org/10.1007/s00382-015-2765-0>.
10. Bothe, O.; Fraedrich, K.; Zhu, X. Precipitation Climate of Central Asia and the Large-Scale Atmospheric Circulation. *Theor. Appl. Climatol.* **2012**, *108*, 345–354. <https://doi.org/10.1007/s00704-011-0537-2>.
11. Peng, D.; Zhou, T.; Zhang, L.; Wu, B. Human Contribution to the Increasing Summer Precipitation in Central Asia from 1961 to 2013. *J. Clim.* **2018**, *31*, 8005–8021. <https://doi.org/10.1175/JCLI-D-17-0843.1>.

12. Chen, C.; Zhang, X.; Lu, H.; Jin, L.; Du, Y.; Chen, F. Increasing Summer Precipitation in Arid Central Asia Linked to the Weakening of the East Asian Summer Monsoon in the Recent Decades. *Int. J. Climatol.* **2021**, *41*, 1024–1038. <https://doi.org/10.1002/joc.6727>.
13. Wei, W.; Zhang, R.; Wen, M.; Yang, S. Relationship between the Asian Westerly Jet Stream and Summer Rainfall over Central Asia and North China. *J. Clim.* **2017**, *30*, 537–552.
14. Chen, F.H.; Huang, W.; Jin, L.Y.; Chen, J.H.; Wang, J.S. Spatiotemporal Precipitation Variations in the Arid Central Asia in the Context of Global Warming. *Sci. China Earth Sci.* **2011**, *54*, 1812–1821. <https://doi.org/10.1007/s11430-011-4333-8>.
15. Yang, K.; Wang, C.; Bao, H. Contribution of Soil Moisture Variability to Summer Precipitation in the Northern Hemisphere. *J. Geophys. Res. Atmos.* **2016**, *121*, 12,108–112,124. <https://doi.org/10.1002/2016JD025644>.
16. Vaid, B.H.; San Liang, X. Tropospheric Temperature Gradient and Its Relation to the South and East Asian Precipitation Variability. *Meteorol. Atmos. Phys.* **2015**, *127*, 579–585. <https://doi.org/10.1007/s00703-015-0385-1>.
17. Vaid, B.H.; Liang, X.S. The Changing Relationship between the Convection over the Western Tibetan Plateau and the Sea Surface Temperature in the Northern Bay of Bengal. *Tellus Ser. A Dyn. Meteorol. Oceanogr.* **2018**, *70*, 1–9. <https://doi.org/10.1080/16000870.2018.1440869>.
18. Vaid, B.H.; Liang, X.S. An Abrupt Change in Tropospheric Temperature Gradient and Moisture Transport Over East Asia in the Late 1990s. *Atmos. - Ocean* **2018**, *56*, 268–276. <https://doi.org/10.1080/07055900.2018.1429381>.
19. Vaid, B.H.; Liang, X.S. The Out-of-Phase Variation in Vertical Thermal Contrast Over the Western and Eastern Sides of the Northern Tibetan Plateau. *Pure Appl. Geophys.* **2019**, *176*, 5337–5348. <https://doi.org/10.1007/s00024-019-02268-3>.
20. Vaid, B.H.; Liang, X.S. Influence of Tropospheric Temperature Gradient on the Boreal Wintertime Precipitation over East Asia. *Terr. Atmos. Ocean. Sci.* **2019**, *30*, 161–170. <https://doi.org/10.3319/TAO.2018.10.24.01>.
21. Vaid, B.H.; Liang, X.S. Effect of Upper Tropospheric Vertical Thermal Contrast Over the Mediterranean Region on Convection over the Western Tibetan Plateau during ENSO Years. *Atmos. Ocean* **2020**, *58*, 98–109. <https://doi.org/10.1080/07055900.2020.1751048>.
22. Vaid, B.H.; Kripalani, R.H. Monsoon 2020: An Interaction of Upper Tropospheric Thermodynamics and Dynamics Over the Tibetan Plateau and the Western Pacific. *Pure Appl. Geophys.* **2021**, *178*, 3645–3654. <https://doi.org/10.1007/s00024-021-02844-6>.
23. Vaid, B.H.; Kripalani, R.H. Strikingly Contrasting Indian Monsoon Progressions during 2013 and 2014: Role of Western Tibetan Plateau and the South China Sea. *Theor. Appl. Climatol.* **2021**, *144*, 1131–1140. <https://doi.org/10.1007/s00704-021-03590-4>.
24. Vaid, B.H.; Kripalani, R.H. Upper Vertical Thermal Contrast Over Western North Pacific and Its Impact on the East Side of Tibetan Plateau During ENSO Years. *Atmos. Ocean* **2022**, *60*, 13–22. <https://doi.org/10.1080/07055900.2022.2060180>.
25. Vaid, B.H.; Kripalani, R.H. Upper Vertical Thermal Contrast over the Western Tibetan Plateau and Its Impact on Convection over the Mediterranean Region during ENSO Events. *Meteorol. Atmos. Phys.* **2022**, *134*, 1–10. <https://doi.org/10.1007/s00703-022-00872-y>.
26. Hansen, J.; Sato, M.; Nazarenko, L.; Ruedy, R.; Lacis, A.; Koch, D.; Tegen, I.; Hall, T.; Shindell, D.; Santer, B.; et al. Climate Forcings in Goddard Institute for Space Studies SI2000 Simulations. *J. Geophys. Res. Atmos.* **2002**, *107*, ACL 2-1–ACL 2-37. <https://doi.org/10.1029/2001JD001143>.
27. Liu, X.; Yanai, M. Relationship between the Indian Monsoon Rainfall and the Tropospheric Temperature over the Eurasian Continent. *Q. J. R. Meteorol. Soc.* **2001**, *127*, 909–937. <https://doi.org/10.1002/qj.49712757311>.
28. Zhou, B.; Zhao, P. Influence of the Asian-Pacific Oscillation on Spring Precipitation over Central Eastern China. *Adv. Atmos. Sci.* **2010**, *27*, 575–582. <https://doi.org/10.1007/s00376-009-9058-7>.
29. Zuo, Z.; Yang, S.; Kumar, A.; Zhang, R.; Xue, Y.; Jha, B. Role of Thermal Condition over Asia in the Weakening Asian Summer Monsoon under Global Warming Background. *J. Clim.* **2012**, *25*, 3431–3436. <https://doi.org/10.1175/JCLI-D-11-00742.1>.
30. Colman, R. On the Vertical Extent of Atmospheric Feedback. *Clim. Dyn.* **2001**, *17*, 391–405. <https://doi.org/10.1007/s003820000111>.
31. Hartmann, D.L.; Larson, K. An Important Constraint on Tropical Cloud–Climate Feedback. *Geophys. Res. Lett.* **2002**, *29*, 12–14. <https://doi.org/10.1029/2002GL015835>.
32. Bony, S.; Colman, R.; Kattsov, V.M.; Allan, R.P.; Bretherton, C.S.; Dufresne, J.L.; Hall, A.; Hallegatte, S.; Holland, M.M.; Ingram, W.; et al. How Well Do We Understand and Evaluate Climate Change Feedback Processes? *J. Clim.* **2006**, *19*, 3445–3482. <https://doi.org/10.1175/JCLI3819.1>.
33. Udelhofen, P.M.; Hartmann, D.L. Influence of Tropical Cloud Systems on the Relative Humidity in the Upper Troposphere. *J. Geophys. Res. Atmos.* **1995**, *100*, 7423–7440. <https://doi.org/10.1029/94JD02826>.
34. Fu, R.; Dickinson, R.E.; Newkirk, B. Response of the Upper Tropospheric Humidity and Moisture Transport to Changes of Tropical Convection. A Comparison between Observations and a GCM over an ENSO Cycle. *Geophys. Res. Lett.* **1997**, *24*, 2371–2374. <https://doi.org/10.1029/97GL02505>.
35. Hirasawal, N.; Kato, K.; Takeda, T. Abrupt Change in the Characteristics of the Cloud Zone in Subtropical East Asia around the Middle of May. *J. Meteorol. Soc. Japan* **1995**, *73*, 221–239. https://doi.org/10.2151/jmsj1965.73.2_221.
36. Chen, T.-C.; Chen, J. An Observational Study of the South China Sea Monsoon during the 1979 Summer: Onset and Life Cycle. *Mon. Weather Rev.* **1995**, *123*, 2295–2318.
37. Cannon, A.J.; McKendry, I.G. Forecasting All-India Summer Monsoon Rainfall Using Regional Circulation Principal Components: A Comparison between Neural Network and Multiple Regression Models. *Int. J. Climatol.* **1999**, *19*, 1561–1578. [https://doi.org/10.1002/\(SICI\)1097-0088\(19991130\)19:14<1561::AID-JOC434>3.0.CO;2-3](https://doi.org/10.1002/(SICI)1097-0088(19991130)19:14<1561::AID-JOC434>3.0.CO;2-3).
38. Parthasarathy, B.; Diaz, H.F.; Eischeid, J.K. Prediction of All-India Summer Monsoon Rainfall with Regional and Large-Scale

- Parameters. *J. Geophys. Res. Atmos.* **1988**, *93*, 5341–5350. <https://doi.org/10.1029/JD093iD05p05341>.
39. Kanamitsu, M.; Ebisuzaki, W.; Woollen, J.; Yang, S.K.; Hnilo, J.J.; Fiorino, M.; Potter, G.L. NCEP-DOE AMIP-II Reanalysis (R2). *Bull. Am. Meteorol. Soc.* **2002**, *83*, 1631–1643. <https://doi.org/10.1175/bams-83-11-1631>.
 40. Kalnay, E.; Kanamitsu, M.; Kistler, R.; Collins, W.; Deaven, D.; Gandin, L. The NCEP / NCAR 40-Year Reanalysis Project. *Bull. Am. Meteorol. Soc.* **1996**, *77*, 437–472.
 41. Liléo, S.; Petrik, O. Investigation on the Use of NCEP/NCAR, MERRA and NCEP/CFSR Reanalysis Data in Wind Resource Analysis. In Proceedings of the European Wind Energy Conference & Exhibition 2011 (EWEC 2011), Brussels, Belgium, 14–17 March 2011; pp. 181–185.
 42. Lu, C.; Zhou, B.; Ding, Y. Decadal Variation of the Northern Hemisphere Annular Mode and Its Influence on the East Asian Trough. *J. Meteorol. Res.* **2016**, *30*, 584–597. <https://doi.org/10.1007/s13351-016-5105-3>.
 43. Zhou, T.; Song, F.; Ha, K.; Chen, X. Decadal Change of East Asian Summer Monsoon: Contributions of Internal Variability and External Forcing. In *The Global Monsoon System: Research and Forecast*; World Scientific: Singapore, 2017.
 44. Li, S.; Gong, Z.; Zhang, S.; Yang, J.; Qiao, S.; Feng, G. Decadal Variation of the Precipitation Relationship between June and August over South China and Its Mechanism. *Clim. Dyn.* **2022**, *59*, 1863–1882. <https://doi.org/10.1007/s00382-021-06073-4>.
 45. Zhao, T.; Fu, C. Comparison of Products from ERA-40, NCEP-2, and CRU with Station Data for Summer Precipitation over China. *Adv. Atmos. Sci.* **2006**, *23*, 593–604. <https://doi.org/10.1007/s00376-006-0593-1>.
 46. Rienecker, M.M.; Suarez, M.J.; Gelaro, R.; Todling, R.; Bacmeister, J.; Liu, E.; Bosilovich, M.G.; Schubert, S.D.; Takacs, L.; Kim, G.K.; et al. MERRA: NASA’s Modern-Era Retrospective Analysis for Research and Applications. *J. Clim.* **2011**, *24*, 3624–3648. <https://doi.org/10.1175/JCLI-D-11-00015.1>.
 47. Liang, X.S. Unraveling the Cause-Effect Relation between Time Series. *Phys. Rev. E—Stat. Nonlinear Soft Matter Phys.* **2014**, *90*, 052150. <https://doi.org/10.1103/PhysRevE.90.052150>.
 48. Liang, X.S. Causation and Information Flow with Respect to Relative Entropy. *Chaos An Interdiscip. J. Nonlinear Sci.* **2018**, *28*, 75311. <https://doi.org/10.1063/1.5010253>.
 49. Liang, X.S. Information Flow and Causality as Rigorous Notions Ab Initio. *Phys. Rev. E* **2016**, *94*, 052201. <https://doi.org/10.1103/PhysRevE.94.052201>.
 50. Liang, X.S. Normalizing the Causality between Time Series. *Phys. Rev. E—Stat. Nonlinear, Soft Matter Phys.* **2015**, *92*, 022126. <https://doi.org/10.1103/PhysRevE.92.022126>.
 51. England, M.H.; McGregor, S.; Spence, P.; Meehl, G.A.; Timmermann, A.; Cai, W.; Gupta, A.S.; McPhaden, M.J.; Purich, A.; Santoso, A. Recent Intensification of Wind-Driven Circulation in the Pacific and the Ongoing Warming Hiatus. *Nat. Clim. Change* **2014**, *4*, 222–227. <https://doi.org/10.1038/nclimate2106>.
 52. Ying, L.; Shen, Z.; Piao, S. The Recent Hiatus in Global Warming of the Land Surface: Scale-Dependent Breakpoint Occurrences in Space and Time. *Geophys. Res. Lett.* **2015**, *42*, 6471–6478. <https://doi.org/10.1002/2015GL064884>.
 53. Shangquan, M.; Wang, W.; Jin, S. Variability of Temperature and Ozone in the Upper Troposphere and Lower Stratosphere from Multi-Satellite Observations and Reanalysis Data. *Atmos. Chem. Phys.* **2019**, *19*, 6659–6679. <https://doi.org/10.5194/acp-19-6659-2019>.
 54. Steiner, A.K.; Ladstädter, F.; Randel, W.J.; Maycock, A.C.; Fu, Q.; Claud, C.; Gleisner, H.; Haimberger, L.; Ho, S.P.; Keckhut, P.; et al. Observed Temperature Changes in the Troposphere and Stratosphere from 1979 to 2018. *J. Clim.* **2020**, *33*, 8165–8194. <https://doi.org/10.1175/JCLI-D-19-0998.1>.
 55. Webster, P.J.; Magaña, V.O.; Palmer, T.N.; Shukla, J.; Tomas, R.A.; Yanai, M.; Yasunari, T. Monsoons: Processes, Predictability, and the Prospects for Prediction. *J. Geophys. Res. Ocean.* **1998**, *103*, 14451–14510. <https://doi.org/10.1029/97jc02719>.
 56. Holton, J.R.; Hakim, G.J. *An Introduction to Dynamic Meteorology*; 5th ed.; Elsevier: Amsterdam, The Netherlands, 2012; Vol. 9780123848; ISBN 9780123848666.
 57. Anber, U.; Wang, S.; Sobel, A. Response of Atmospheric Convection to Vertical Wind Shear: Cloud-System-Resolving Simulations with Parameterized Large-Scale Circulation: Part I: Specified Radiative Cooling. *J. Atmos. Sci.* **2014**, *71*, 2976–2993. <https://doi.org/10.1175/JAS-D-13-0320.1>.
 58. Wu, W.; Liu, Y.; Jensen, M.P.; Toto, T.; Foster, M.J.; Long, C.N. A Comparison of Multiscale Variations of Decade-Long Cloud Fractions from Six Different Platforms over the Southern Great Plains in the United States. *J. Geophys. Res. Atmos.* **2014**, *119*, 3438–3459. <https://doi.org/10.1002/2013JD019813>.
 59. Branstator, G. Circumglobal Teleconnections, the Jet Stream Waveguide, and the North Atlantic Oscillation. *J. Clim.* **2002**, *15*, 1893–1910. [https://doi.org/10.1175/1520-0442\(2002\)015<1893:CTTJSW>2.0.CO;2](https://doi.org/10.1175/1520-0442(2002)015<1893:CTTJSW>2.0.CO;2).
 60. Li, J.; Yu, R.; Zhou, T. Teleconnection between NAO and Climate Downstream of the Tibetan Plateau. *J. Clim.* **2008**, *21*, 4680–4690. <https://doi.org/10.1175/2008JCLI2053.1>.

Disclaimer/Publisher’s Note: The statements, opinions and data contained in all publications are solely those of the individual author(s) and contributor(s) and not of MDPI and/or the editor(s). MDPI and/or the editor(s) disclaim responsibility for any injury to people or property resulting from any ideas, methods, instructions or products referred to in the content.